IEEE Access
Multidisciplinary | Rapid Review | Open Access Journal

Received 17 May 2023, accepted 9 June 2023, date of publication 20 June 2023, date of current version 3 July 2023.

Digital Object Identifier 10.1109/ACCESS.2023.3288017

RESEARCH ARTICLE

Automated Segmentation of Brain Tumor MRI Images Using Deep Learning

SURENDRAN RAJENDRAN[1], SURESH KUMAR RAJAGOPAL[2], TAMILVIZHI THANARAJAN[3], K. SHANKAR[1,4], (Senior Member, IEEE), SACHIN KUMAR[4], (Senior Member, IEEE), NAJAH M. ALSUBAIE[5], MOHAMAD KHAIRI ISHAK[6], (Member, IEEE), AND SAMIH M. MOSTAFA[7,8]

[1]Department of Computer Science and Engineering, Saveetha School of Engineering, Saveetha Institute of Medical and Technical Sciences, Chennai 602105, India
[2]Center for System Design, Chennai Institute of Technology, Chennai 600069, India
[3]Department of Computer Science and Engineering, Panimalar Engineering College, Chennai 600123, India
[4]Big Data and Machine Learning Laboratory, South Ural State University, 454080 Chelyabinsk, Russia
[5]Department of Computer Sciences, College of Computer and Information Sciences, Princess Nourah bint Abdulrahman University, Riyadh 11671, Saudi Arabia
[6]School of Electrical and Electronic Engineering, Engineering Campus, Universiti Sains Malaysia, Penang 14300, Malaysia
[7]Computer Science Department, Faculty of Computers and Information, South Valley University, Qena 83523, Egypt
[8]Faculty of Industry and Energy Technology, New Assiut Technological University (N.A.T.U.), Assiut 71515, Egypt

Corresponding author: Najah M. Alsubaie (Nmoalsubaie@pnu.edu.sa)

This research was funded by Princess Nourah bint Abdulrahman University Researchers Supporting Project number (PNURSP2023R321), Princess Nourah bint Abdulrahman University, Riyadh, Saudi Arabia.

ABSTRACT Segmenting brain tumors automatically using MR data is crucial for disease investigation and monitoring. Due to the aggressive nature and diversity of gliomas, well-organized and exact segmentation methods are used to classify tumors intra-tumorally. The proposed technique uses a Gray Level Co-occurrence matrix extraction of features approach to strip out unwanted details from the images. In comparison with the current state of the art, the accuracy of brain tumor segmentation was significantly improved using Convolutional Neural Networks, which are frequently used in the field of biomedical image segmentation. By merging the results of two separate segmentation networks, the proposed method demonstrates a major but simple combinatorial strategy that, as a direct consequence, yields much more precise and complete estimates. A U-Net and a Three-Dimensional Convolutional Neural Network. These networks are used to break up images into their component parts. Following that, the prediction was constructed using two distinct models that were combined in a number of ways. In comparison to existing state-of-the-art designs, the proposed method achieves the mean accuracy (%) of 99.40, 98.46, 98.29, precision (%) of 99.41, 98.51, 98.35, F-Score (%) of 99.4, 98.29, 98.46 and sensitivity (%) of 99.39, 98.41, 98.25 for the whole tumor, enhanced tumor, tumor core on the validation set, respectively.

INDEX TERMS Brain tumor, medical imaging, segmentation, three dimensional CNN, U-Net.

I. INTRODUCTION

Brain tumors are one of the most lethal types of cancer and the most frequent worldwide, according to Global Cancer Statistics data collected in 2020 [1]. A majority of primary CNS tumors are found in the brain, accounting for about 90% of all cases. Treatment costs for brain tumors might vary widely depending on the imaging technology used [2]. A patient with a brain tumor may expect to pay $62,602 to increase their life expectancy by 16.3 months [3] using current treatment methods. Patients with brain tumors are dying at a higher rate than ever before, and the five-year survival rate is just 72.5% [4]. CT does not produce as good picture of soft tissue as MRI, but it may be used to characterize the tissue. A range of MR imaging methods, including T1-weighted (T1ce), T1-weighted, T2-weighted, post-contrast, and fluid-attenuated inversion recovery, may be used to segment the brain tumor and the tissues around it (FLAIR) [5]. There are three forms

The associate editor coordinating the review of this manuscript and approving it for publication was Vishal Srivastava.

of tumor necrosis—enhanced necrosis, and edoema [6]—that may be seen in the visual output of MRI modalities. Necrosis, enhancement, and peritumoral edoema are the three tumor areas employed in clinical practice.

According to the World Health Organization, brain tumors are among the most lethal forms of cancer that may occur anywhere in the world. Glial cell carcinogenesis in the spinal cord and brain causes gliomas, the most frequent primary brain tumor. According to the American Cancer Society, the average survival duration for glioblastic cancer patients is less than 14 months following diagnosis [7]. It is possible. In each imaging modality, non-invasive Magnetic Resonance Imaging (MRI), which has been widely used to detect brain malignancies, presents a broad and diverse variety of tissue contrasts [8]. Because the method is tedious and time-consuming, only skilled neuroradiologists can currently segment and analyze structural MRI images of brain tumors [9], [10]. As a consequence of this, it may be challenging to monitor and quantify lesions using a large number of scans and volumes due to the fact that the characteristics of each patient's tumour are unique. Artifacts [11] such as abnormalities, pixel fluctuations, and inconsistencies in homogeneity may also be seen in these photos, which were taken with different scanners. That is why it is vital to have an accurate and fast method of segmenting brain tumors in order to cope with binary (high or low) and several types of risk classes (e.g. low or mild, moderate or high) [12].

For the detection and monitoring of brain tumors, MRI, a typical non-invasive imaging technique, produces high-quality pictures of the brain that are free of skull damage and artefacts [13]. Because of the wide range of variations in size, form, and function across gliomas, it is very difficult to accurately segment them by hand. More accurate and easy diagnosis and therapy may be possible with automated segmentation.

Brain cancer detection necessitates the use of artificial intelligence (AI), which has become a standard strategy for medical diagnostics. It displays tools for generational segmentation. In the first generation of brain lesion segmentation, the conventional technique predominates (BLS). In the second and third generations, AI systems based on machine learning (ML) [14], [15] and deep learning (DL) predominated. ML and DL have different approaches to extract characteristics from instances. Many machine learning (ML) categorization models are built as autonomous analytical learning models that deliver precise predictions based on data properties. Tissue characterization in medical imaging applications has been shown to benefit from machine learning [16]. Radiologists and researchers who use ML approaches [17] are exclusively responsible for picking the most convincing traits, which leads to biased methodologies.

In this study, the authors primarily suggested an MR brain image segmentation model for automatically segmenting brain tumors [18]. Convolutional neural network (CNN) techniques, which are machine learning pipeline approaches that focus on the biological processes of synapses and neurons, have garnered a lot of attention (connections). Afterward, they conducted a literature search to find an example pipeline for categorizing brain tumors using CNNs. Using CNNs, they go into the future to research radionics, a new area of study. Treatment response and survival may be predicted by looking at the quantitative properties of brain tumors such as signal intensity, form, and texture. Structural multimodal magnetic resonance imaging was used by Pei et al. [19] to develop a deep learning system for classifying brain tumors and predicting their long-term stability (MRIs). As a starting point, they proposed using 3D context-aware deep learning to analyze MRI image subzones for tumor categorization. So to determine more about the subtype of tumor, they use a standard 3D CNN.

Recent years have seen a rise in interest in network architectures like FCN and U-net. Due to the excellent performance it offers, it has become the most often used architecture among them. Recently, the U-Net architecture has been recognised as a genetic solution strategy for the difficulties that are present in biomedical imaging data research [20]. In contrast, U-Net has a lower output resolution than its input resolution since it does not use convolution with padding. This results in a lower overall resolution. As a result, if we need the output resolution to match the input resolution, we can't use U-Net. A further benefit of the U-Net design is that it progressively recovers down sampled picture and shares low-level characteristics from shallow layers with deeper ones. As a consequence of the information distortion generated by this direct information relationship, the final prediction is warped. The capacity to better separate brain tumors may be enhanced if an information bridge between the shallow and deep levels works well. Unlike the U-Net design, W-Net employs a two-stage U-Net for its architecture. Although W-Net includes a lot of trainable parameters, it is difficult to train the model because of this. MIRAU-Net, or the Residual Attention U-Net.

The suggested Inception-Res block replaces the original U-Net model's encoder and decoder layers' sequence of two convolutional layers. New skip paths, such as the Inception-Res skip link, are also introduced. Small-scale tumors may be accurately segmented during the upsampling phase by providing appropriate spatial information and situating low-level feature maps utilizing attention gates.

As a result of the loss of local information and the consolidation of finer contextual information at the decoder's sampling layer, a skip connection recaught the characteristics previously collected in the related encoder. Each max-pooling layer loses part of its information when it is down sampled. When implementing the skip connection, the depth concatenation layer is used.

II. RELATED WORK

A patch-based approach is detailed in the analyses of the brain and the detection of tumors by neural networks with deep convolutional layers in regard to identifying brain tumors

in MRI scans. To begin, N patches are used to divide the MRI image. The center pixel label of each patch is then estimated using a trained CNN model. Finally, the forecasts for all patches are merged to achieve the total results. The classification system implements the idea of deep transfer learning and takes use of a GoogLe net that has already been trained to extract characteristics from MRI scans of the brain. In order to categorise the retrieved characteristics, tried-and-true classifier models are included. An MRI dataset obtained from figshare is used as the basis for the experiment, which employs a patient-level five-fold cross-validation procedure. This system achieves a mean accuracy of classification of 98%, which is superior than all other systems that are considered state-of-the-art [21].

One of the three pathogenic kinds of brain tumors, Brain Tumor Classification using CNN (BTCCNN), has been established using an accurate and automated classification technique (glioma, pituitary tumor and meningioma). To extract features from brain MRI images, a deep transfer learning CNN model is used. Known classifiers are used to sort the extracted characteristics into different groups. Afterwards, the whole system is thoroughly inspected. The suggested technique had the greatest classification performance of all similar articles [22] when evaluated on the publicly accessible dataset.

3D Incremental Deep Convolutional Neural Network models were built for entirely automated segmentation of brain tumors. Instead of following a predetermined path to identify the optimal hyper parameters, these models use a trial-and-error strategy to do so. Using ensemble learning, a more efficient model may be built [23]. A novel training approach for CNN models was proposed to address the challenge of training CNN models by limiting and setting an upper limit on the most critical hyper parameters.

In order to classify and segment the three distinct types of brain tumors, which are pituitary tumors, meningiom's, and gliomas, it was not necessary to perform any data preprocessing on the input images in order to delete vertebral or skull column components prior to analyzing the MRI images. This was the case because it was not necessary to do any preprocessing on the input images. An MRI dataset from 230 patients, including 3064 slices, was used to evaluate the method's performance against previously published traditional machine learning and deep learning techniques [24].

III. AUTOMATED SEGMENTATION OF BRAIN TUMOR MRI IMAGES USING DEEP LEARNING (ASBTCNN)

A. GREY LEVEL CO-OCCURANCE MATRIX (GLCM)

To better understand brain tumors, a Gray Level Co-occurrence Matrix combined with a Convolutional Neural Network may be used. In this research, TI1 data from brain cancers such as glioma, meningioma, and pituitary tumor will be used to test the accuracy of a convolutional neural network. The information that is collected from the grey level co-occurrence matrix will be fed into the network. According

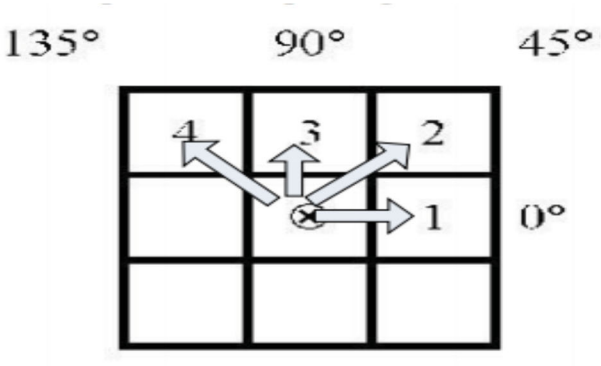

FIGURE 1. GLCM's direction distance.

to the practical application of this study, the results of a Convolutional Neural Network classification show that the contrasting characteristics of the Gray Level Co-occurrence matrix may improve the accuracy by up to 20% in comparison to the other features. By using this extraction characteristic, Convolutional Neural Networks (CNNs) may accelerate the classification process.

In order to get statistical data on the texture of an image, GLCM functions, which determine how often specific pairs of pixels in an image have the same value and are in a predetermined spatial relationship, may be utilized. Fig. 1 depicts an easy-to-understand depiction of direction and distance. Second-order statistical texture characteristics may be extracted using the Level Co-occurrence Matrix (GLCM) technique. For example, third- and higher-order textures look at the interactions between three or more pixels in a scene. As a result, it's common to use fewer shades of grey.

Three-dimensional GLCM plots have been developed, compared, and discussed for a variety of acquired pictures. In addition, the GLCMs were used to compute and compare statistical metrics (such as the matrix's maximum occurrence, location, and standard deviation) with the arithmetic average roughness Ra. There's also a brand-new parameter for measuring surface roughness, termed the maximum width of the matrix.

B. VANTAGE POINT TREE (VPT)

Rarely, but effectively, VP-trees have been employed in applications such as picture indexing [25] and music information retrieval [26]. These algorithms have shown excellent picture patch retrieval performance when using the L2 metric [27]. VP-Good Tree's findings prompted us to look at additional distortion measures, which may be better suited for multimedia aspects than the Euclidian metric. A significant portion of these metrics is made up of Bregman divergences, which are not measures in and of themselves and do not fulfil the conditions of the triangle inequality.

This method can be used to find the closest neighbor of an object x. Recursion is used in the search process. Nodes in the tree have vantage points and threshold distances, and we use these values to guide our decisions at each stage. The

point of interest x will be a long distance away from where you are. If the distance d is less than the threshold t, then the algorithm should be used iteratively to search the sub tree of the node, which includes the points that are near the point of view. If the distance d is greater than the threshold t, then the algorithm should be used recursively to search the sub tree of the node, which includes the points that are further from the point of view. It is impossible to search the other sub tree of this node when the algorithm discovers a nearby point n with a distance x smaller than |t, d|, hence the found node n is returned. Recursive searching of the other sub tree is required if the first search fails.

At first, the similarity matrix is presented in the form of the symmetric matrix denoted by "D." The following mathematical formulation explains how to determine the degree of the kth data point in a high-dimensional dataset.

$$M_k = \sum_{k,l=1}^{n} D_{k,l} \tag{1}$$

The similarity matrix between two (i.e., uk and Ul) data points taken from highly populated high-dimensional data is denoted by the letter $D_{k,}$l, which comes from equation (1). The letter 'Mk' signifies the size of the 'kth' data point.

In spectral clustering, the Gaussian kernel function is the method utilised to determine the similarity score between two data points. The formula for this function is as follows:

$$D(k,l) = exp\frac{-\|U_k - U_L\|^2}{2\sigma^2} \; if \; k \neq l \; and \; D_{k,k} = 0 \tag{2}$$

The Euclidean distance between two data points, Uk and Ul, is represented by the value $\|U_k - U_l\|^2$ in equation (2). A similarity matrix is built for each data point based on this equation. In this case, the width of the neighborhood is controlled by the parameter σ. The unnormalized Laplacian matrix is produced using data points and is provided by the diagonal matrix has been obtained.

$$\mathrm{L} = \mathrm{DI} - \mathrm{M} \tag{3}$$

Based on equation (3), "L" refers to the Laplacian matrix, "DI" stands for the diagonal matrix, and "M" stands for the similarity matrix.

Fig. 2 depicts a two-dimensional vantage point tree. The procedure is as follows: All points are given to the root node first. Following that, a random vantage point (R) is chosen (Figure 2a). By dividing the points into two equal halves (a = 5), the threshold is computed. All d points migrate to the left sub tree (p, s q), while the remaining ones (u, t, v w) move to the right (u, t, v w) (Figure 2b). The child node that is most directly responsible for the problem is given priority. A second VP is chosen at random (u = 4). Finally, all points that are "d" shift to the left sub tree (t), while the remaining points are moved right (v-p). This completes the process (v, w) (Figure 2c). In the last step, the left node is dealt with. One of the VPs is picked at random (p equals 6). As a result, for all points where d (Poin; v, p) (Figure 2d), s will take over as the left subtree and q will take over as the right subtree.

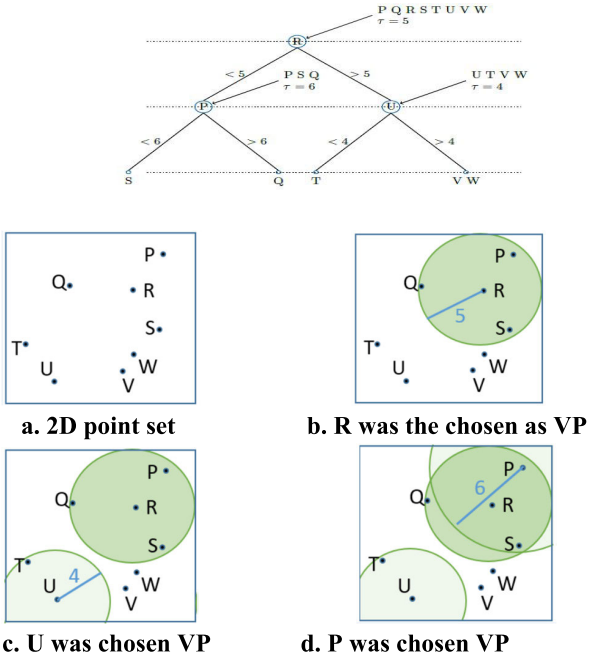

FIGURE 2. Vantage point tree construction.

C. D-CNN (CONVOLUTION NEURAL NETWORK)

Convolution filters, pooling layers, and a feed-forward neural network are all part of this CNN classification system. The suggested CNN classification algorithm's internal architecture is represented in this diagram. This suggested CNN architecture contains two convolutional layers, two pooling layers, and one preprocessed by data augmentation layer. In this case, the right shift is A. B, reverse the image. C a shift to the left fully connected neural networks are proposed in the proposed CNN architecture for brain image categorization as shown in Figure 3. The input brain picture is convolved with the convolutional kernel of the first convolutional layer, which includes 128 convolutional filters. In the first convolutional layer, the kernel is 3×3.

It is not possible to directly apply the high-definition pixels produced by each convolution filter to feed-forward neural networks. As a consequence of this, the data that is produced by the output of each convolution filter needs to be compressed before it is fed into neural networks. Pooling layers may be used to accomplish this. In the CNN architecture, there are two kinds of pooling layers: average pooling and max pooling.

Average pooling layers use the average value of the 2×2 filter masks to choose an output response from a convolution filter. On the output response of the convolution filter, the max-pooling layer additionally locates a 2×2 pixel mask and selects the maximum value. The suggested CNN architecture employs a max-pooling layer since it has a high degree of accuracy.

The following is a mathematical phrase that may be constructed to represent the output value γ at the location (x, y,

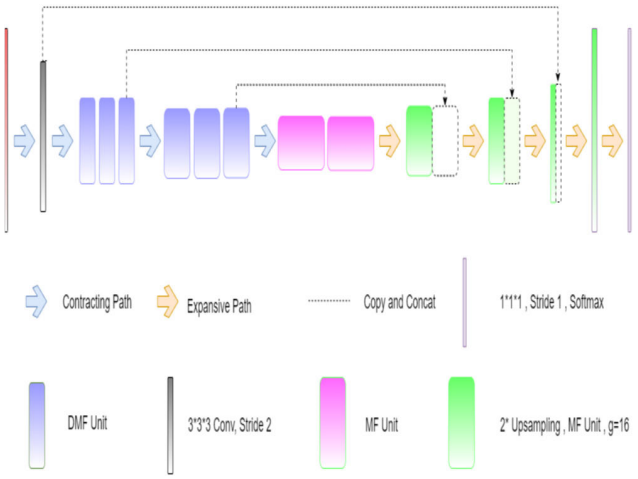

FIGURE 3. Architecture 3 D-Convolution neural network.

z) on the jth feature map in the ith 3D convolutional layer:

$$\gamma^{i}_{j,xyz} = \mathrm{ReLU}(b^{(i)}_{j} + \sum_{m=1}^{M^{(i-1)}} \sum_{u=0}^{U^{(i)}-1} \sum_{v=0}^{V^{(i)}-1} \sum_{w=0}^{W-1} \times w^{(i)}_{jm,pqr} \gamma^{(i-1)}_{m,(x+p)(y+q)(z)+r}) \quad (4)$$

where ReLU(·) represents elementwise ReLU function; $b^{(i)}_{j}$ is the shared bias for jth process region; $w^{(i)}_{jm,uvw}$ is the (u, v, w) th data of the 3D filter for the jth process region at the ith layer related with the mth process region in the (i-1)th layer.

Tensor operations may be used to explain simply the link between two neighboring layers (in this case from (i-1)th to ith, as given by.

$$\gamma^{(i)} = \sigma\left(W^{(i)}\gamma^{(i-1)} + b^{(i)}\right) \quad (5)$$

where $\gamma^{(i)}$ and $\gamma^{(i-1)}$ are the output and input for the ith layer; σ (·) represents the activation function performing element wise;

This is the loss function, which is defined as the mean squared error between a 3D-prediction CNN's and the ground truth of the training dataset.

$$L\left(W, b/D\right) = \frac{1}{n}\sum_{k=1}^{n}\sum_{l=1}^{12}\left(y^{truth}_{kl} - y^{pred}_{kl}\right)^2 \quad (6)$$

where D is the trained data set $\{x_k, y_k\}$, n represents the quantity of samples, and l signifies the efficient property vector of the component index. The optimal parameters $\{W^{*}\ and\ b^{*}\}$ may be derived by minimizing the loss function, which is the inverse of the loss function,

$$\left\{W^{*}, b^{*}\right\} = argmin_{\{W,b\}}\left\{\mathcal{L}\left(W, b/D\right)\right\} \quad (7)$$

In DNN-based techniques, a recurring problem is how to limit the overfitting that occurs as a result of the DNN's exceptional approximation capacity.

1) CONVOLUTIONAL LAYER

In this layer, convolutional kernels or filters transform pictures into feature map data. Kernels of data (height, length, and depth) flow across three dimensions in a 3D CNN, creating 3D maps. It is essential to use a 3D CNN to analyze data that has a temporal or volumetric context.

2) POOLING LAYER

On the convolution output, down-sampling or pooling is done. As a filter passes over the convoluted output, it takes the average value, weighted average, and/or the maximum value. It is the purpose of the pooling the layer to gradually lower the spatial size of the matrix in order to minimize the number of parameters and to control over fitting of the model.

3) FULLY-CONNECTED LAYER

Convolution and pooling findings are used to categories the picture into a label, the primary purpose of a fully connected layer. To obtain probabilities, a softmax function is utilized that pushes values between 0 and 1 in this layer. Batch normalization is used to speed up training and limit the risk of overfitting.

Chanel originally created the 3D CNN model, which is the first model to be utilized in the ensemble. In order to provide a feature representation at many different scales for volumetric segmentation, weighted dilated convolutions are used in a multitier unit.

a: PRE-PROCESSING

A number of techniques are used to augment the data in order to ensure its accuracy before it is included in the training network (cropping, rotation, mirroring). During training, we used 150 epochs of training time, a 128 × 128 patch size, and a modified loss function that included the generalized dice and focused losses into one loss function. The hyper parameters have been fine-tuned.

b: INFERENCE

We used zero-padding to reduce the voxels in the MRI data from 240 240 155 to 240 240 160 a depth that can be divided by the network. We make utilize the training network to create probabilistic maps if the data are of a quality that allows for inference to be drawn from them. Following that, the ensemble relies its final prediction on the information provided by these maps.

D. U-NET

Segmentation of meaning using U-Net is possible. As the name suggests, it has two distinct paths. A convolutional network's contracting route follows the usual design. For downsampling, a 2 × 2 max pooling operation with stride two is used after each convolution, followed by a rectified linear unit (ReLU), as shown in Fig. 4. Every time a sampling step is taken, the number of feature channels increases by one. In the expanding path of the algorithm, some of the processes

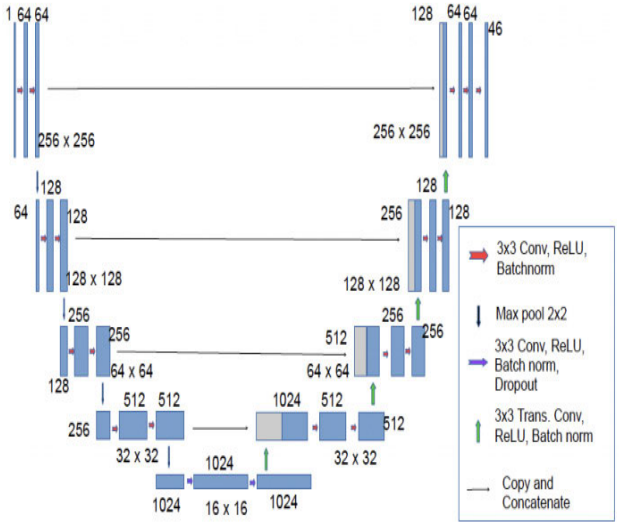

FIGURE 4. Architecture of 3D U-Net.

include up-sampling the extracted features, concatenating it with the cropped feature map that was generated by the contracting route, and then performing convolution of two 3×3 feature channels each followed by a ReLU. Because each iteration of the convolution algorithm results in the loss of some border pixels, cropping is necessary. The last layer of the neural network model consists of a 1×1 convolution, which is used to translate each 64-component feature representation to the desired number of classes. This network has a maximum of 23 convolutional layers in its architecture.

In the second model of our ensemble, the ReLU activation functions have been switched out for leaky ReLUs, and an instance normalization has taken the place of batch normalization. Both of these changes were made in order to improve performance.

1) PRE-PROCESSING

To minimize the MRI slice's size, crop the data. Next, normalize the z-scores after resampling the pictures and determining the median voxel spaces in the otherwise diverse data.

2) TRAINING

In order to properly train the network, we use 128×128 x 128 voxels with a batch size of 2. Mirroring, rotation, and gamma correction are performed on the data during runtime in order to reduce overfitting and the accuracy of the model's segmentation should be improved. During training, the binary cross-entropy as well as dice are combined in order to do the calculation necessary to determine the loss function.

3) INFERENCE

During the inference process, greater importance is placed on the voxels that are located closer to the centre, which is based on a patch-based approach. Additional data augmentation is provided by mirroring along the patch axes while conducting tests. For each ensemble, a probability map is generated as a result.

The posterior probability of a voxel i being labelled with a certain value l may be computed as follows for each image:

$$p\left(y_i = l / \left(M_i\right)\right) = \frac{e^{f_{yl}(M_i)}}{\sum_{k'=1}^{K} e^{f_{y_{k'}(M_i)}}} \tag{8}$$

where $f_{yi}(\cdot)$ is the CNN computation function, M_i is the patch of the voxel i and k' is the class number. The following is the stated form of the weighted cross-entropy loss function.

$$Loss = -\sum_i log\left(p\left(y_i = groundtruth / X\left(M_i\right)\right)\right) \tag{9}$$

Given the fact that the cross-entropy between the predicted distribution p and the real distribution q is - $\sum_i q\left(y_i\right) log\left(p\left(y_i / X\left(M_i\right)\right)\right)$n and the actual distribution q(yi) is 1 for ground truth and 0 otherwise.

IV. RESULTS AND DISCUSSION

The first stage in the classification procedure was to extract the picture components. It was a dim-level co-event grid surface element extraction approach called Gray Level Co-event Matrix surface element extraction that was used for the extraction of the element. Relationship, divergence, homogeneity, differentiation, and energy on points were all GLCM features that were used (0, 45, 90, and 135).

Fig. 5 depicts four original MRI images that were sent to the GLCM and VPT for processing. Then, using the training picture, the brain tumor is segmented. Dice scores of 3.92, 18.80, and 23.80 are achieved by the suggested technique for enhanced tumor, tumor core, and whole tumor, respectively.

Using VPTs, we are able to locate the files of the test highlight vectors that are closest to our own and extract their names from their markings. This information is used to calculate the likelihood of each mark appearing at each point in the framework based on the available data. It follows that a straight line of marked probability is interspersed all across the whole image. CNN seems to be more successful in segmenting tumors in experiments involving tumor augmentation, according to both qualitative and quantitative data. On the other hand, the U-Net is more precise than other methods in regard to the segmentation of tumor cores. Although both networks do equally well in regard to detecting the whole tumor segmentation on their own, the expectations are taken into account. The most current ensemble projections for the following three areas were generated only using U-output net models, for the purposes of the enhanced tumor, tumor core, and whole tumor, we observed the output.

Fig. 6 and Fig. 7 shows the proposed method ASBTCNN was compared with the existing methods Brain Tumor Analysis and Detection Deep Convolutional Neural Networks (BTADCNN), Brain Tumor Classification Using CNN (BTC-CNN), and Brain Tumor Classification and Segmentation Using a Multiscale CNN (BTCSMCNN) for F-Score and

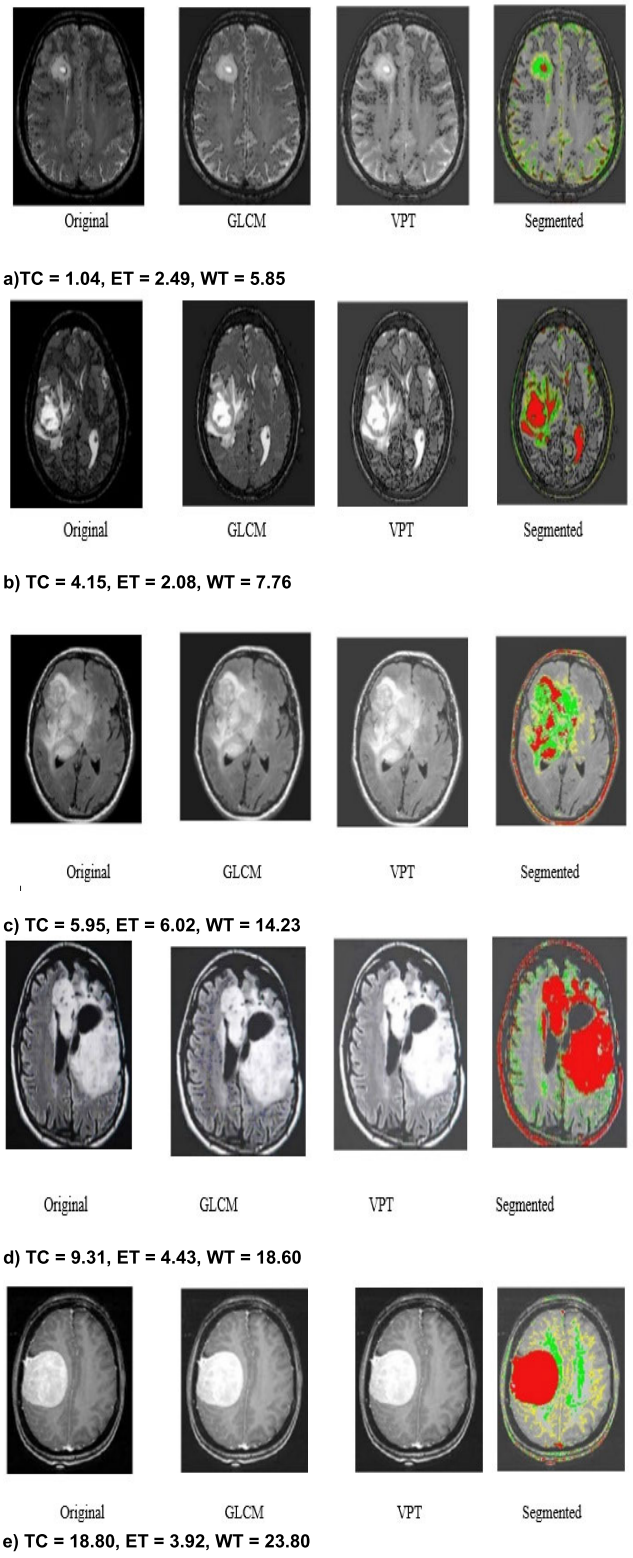

FIGURE 5. GLCM and VPT feature selection and segmentation of the Brain Tumor.

Sensitivity in percentage of Enhanced Tumor. The suggested technique has an F-Score of 98.46 % for enhanced tumors,

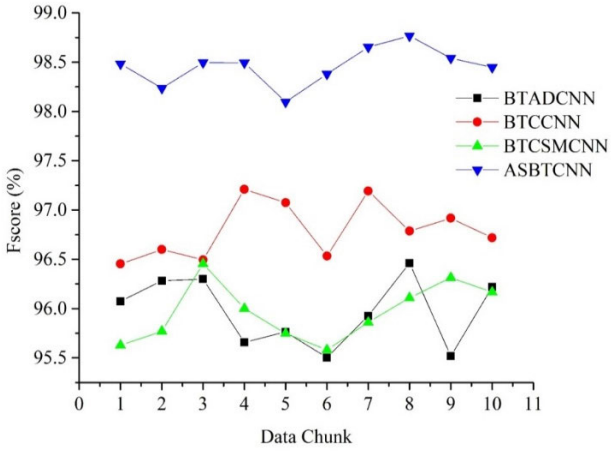

FIGURE 6. F-Score for enhanced tumor in percentage.

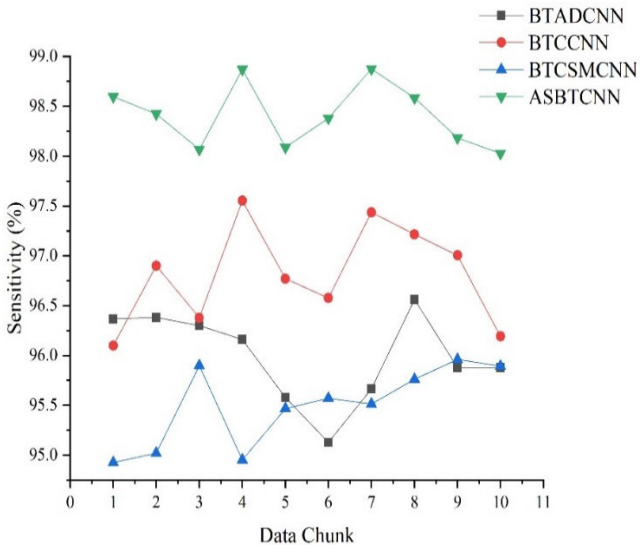

FIGURE 7. Sensitivity for enhanced tumor in percentage.

which is much greater than the prior existing methods of 95.97 %, 96.79 %, and 95.96 %. Similarly, the sensitivity of 98.41 % for Enhanced Tumors in the proposed method is greater than the existing methods of 95.99 % (BTADCNN), 96.81 % (BTCCNN) and 95.49 % (BTCSMCNN).

Fig. 8 and Fig. 9 show the F-Score and Sensitivity in percentage of tumor core for the proposed method ASBTCNN was compared to the existing methods "Brain Tumor Analysis and Detection Deep Convolutional Neural Networks (BTADCNN), Brain Tumor Classification Using CNN (BTCCNN), and Brain Tumor Classification and Segmentation Using a Multiscale CNN (BTCSMCNN). The proposed method has an F-Score of 98.29 % for tumor core, which is much greater than the preceding methods, which had F-Score of 92.74 %, 94.83 %, and 97.99 %. Similarly, the sensitivity of 98.25 % for Tumor Core in the proposed method is greater

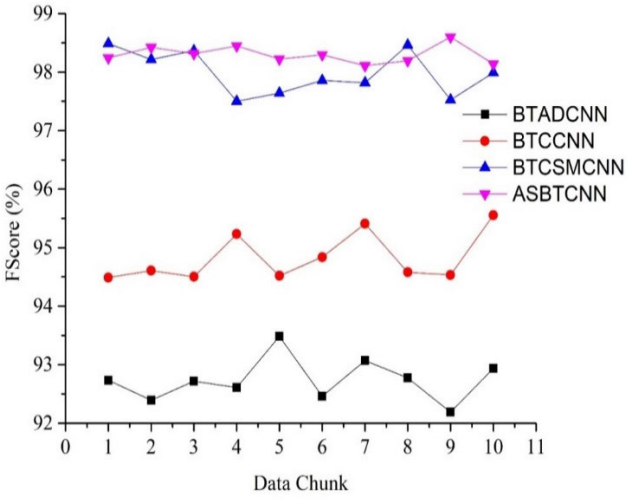

FIGURE 8. F-Score (%) for Tumor core.

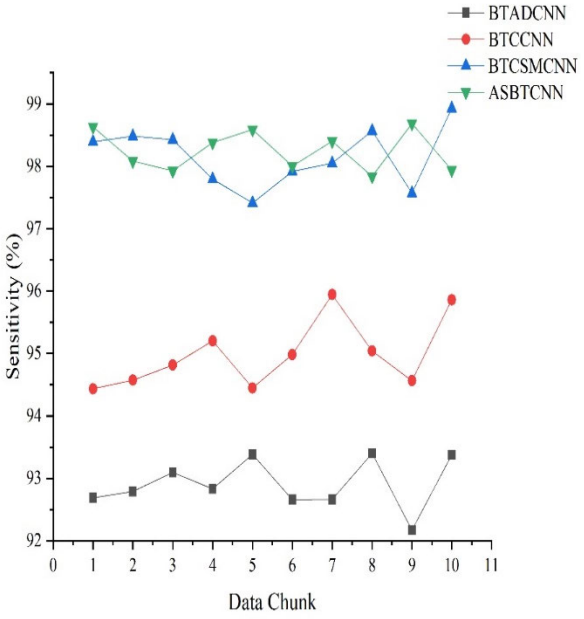

FIGURE 9. Sensitivity (%) for Tumor core.

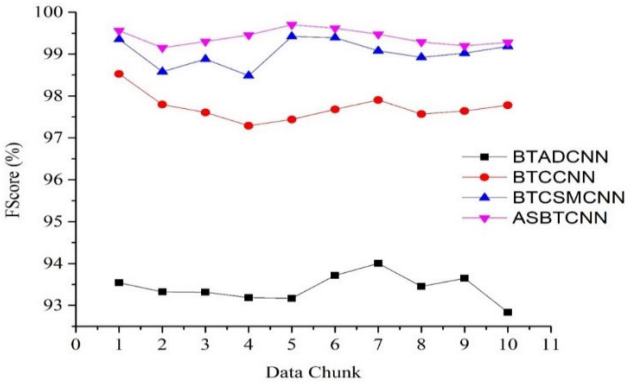

FIGURE 10. F-Score (%) for Whole Tumor.

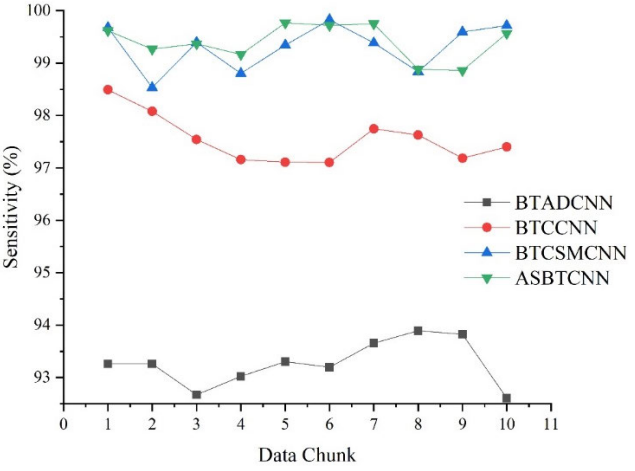

FIGURE 11. Sensitivity (%) for Whole Tumor.

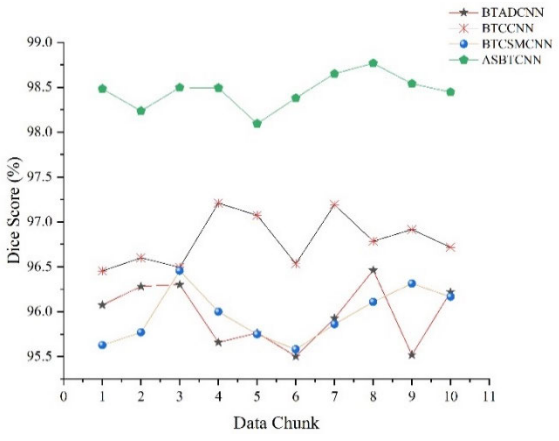

FIGURE 12. Dice score (%) for Enhanced Tumor.

than the existing methods of 92.91 % (BTADCNN), 94.98 % (BTCCNN), and 98.15 % (BTCSMCNN).

Fig. 10 and Fig. 11 show the F-Score and Sensitivity in the percentage of whole tumor for the proposed method ASBTCNN was compared to the existing methods Brain Tumor Analysis and Detection Deep Convolutional Neural Networks (BTADCNN), Brain Tumor Classification Using CNN (BTCCNN), and Brain Tumor Classification and Segmentation Using a Multiscale CNN (BTCSMCNN). The new technique has an F-Score of 99.40 percent for Whole tumors, which is much greater than the preceding methods, that had F-Score of 93.42 %, 97.72 %, and 99.03 %. Similarly, the sensitivity of 99.39 % for Whole Tumor in the proposed method is greater than the existing methods of 93.27 % (BTADCNN), 97.54 % (BTCCNN) and 99.31 % (BTCSMCNN).

Fig. 12, Fig. 13 and Fig. 14 shows the proposed method ASBTCNN was compared with the existing methods Brain Tumor Analysis and Detection Deep Convolutional Neural

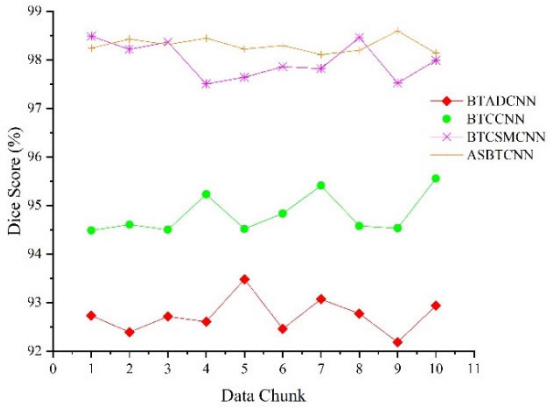

FIGURE 13. Dice score (%) for Tumor Core.

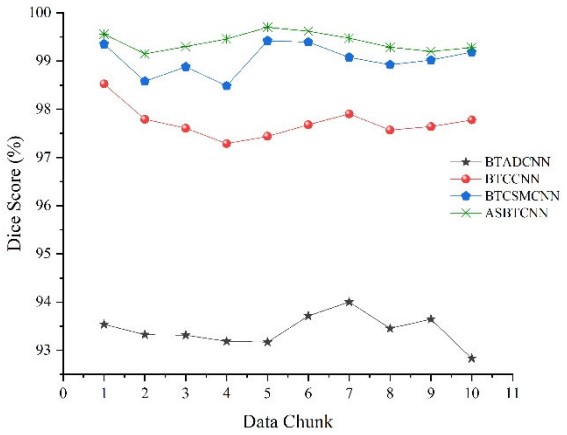

FIGURE 14. Dice score (%) for Whole Tumor.

Networks (BTADCNN), Brain Tumor Classification Using CNN (BTCCNN), and Brain Tumor Classification and Segmentation Using a Multiscale CNN (BTCSMCNN) for Dice Score in percentage of Enhanced Tumor, Tumor Core and Whole Tumor. The suggested technique has the Dice Score of 98.46 % for enhanced tumors, 98.29 % for enhanced tumors, 99.40 percent for Whole tumors, which is much greater than the prior existing methods.

In this proposed method, the performance of our strategy has been compared to all other techniques that were previously available when trying to categorize brain tumors. Our solution outperforms every other method presently in use, according to the comparison. This is to show how successful our technique is despite the fact that we only have a small amount of training data compared to past research. The table only shows the accuracy as a performance criterion since it is used in all other studies. All indicators pointing to the proposed work being better than what is currently being done

V. CONCLUSION

The proposed approach specifies the feature extraction techniques implemented by the GLCM and VPT networks, and a combination of the two networks referred to as the ''ensemble of two networks.'' The problem of segmentation in biological images is often addressed by each of these networks separately, which is a difficult problem to begin with and requires a solution that is capable of handling its complexity. When used in conjunction with an MRI image, the brain tumour ensemble effectively detects brain tumours from normal brain tissue with high accuracy, exceeding predictions from a broad variety of other sophisticated algorithms. We aggregate the model's outputs in order to produce the best potential outcomes, which is accomplished via the use of a process called variable assembly. For disease management and patient care, the proposed ensemble provides a method that is therapeutically favorable and automated for creating brain tumor segmentation. In the proposed method, F-score and sensitivity of 98.29% and 98.25% of Tumor core was achieved. With 99.40 % F-Score and 99.39% Sensitivity, the proposed approach delivered the greatest results for the Whole tumor. This method is both efficient and effective in terms of both the efficiency and efficacy of treatment. Because of this, most state-of-the-art models were able to outperform these three models in terms of F-Score and sensitivity.

DATA AVAILABILITY

The data are available from the corresponding author upon reasonable request.

CONFLICT OF INTEREST

The authors declare that there are no conflicts of interest regarding the publication of this paper.

ACKNOWLEDGMENT

Princess Nourah bint Abdulrahman University Researchers Supporting Project number (PNURSP2023R321), Princess Nourah bint Abdulrahman University, Riyadh, Saudi Arabia.

REFERENCES

[1] H. Sung, J. Ferlay, R. L. Siegel, M. Laversanne, I. Soerjomataram, A. Jemal, and F. Bray, "Global cancer statistics 2020: GLOBOCAN estimates of incidence and mortality worldwide for 36 cancers in 185 countries," *CA, A Cancer J. Clinicians*, vol. 71, no. 3, pp. 209–249, May 2021.
[2] K. K. Farmanfarma, M. Mohammadian, Z. Shahabinia, S. Hassanipour, and H. Salehiniya, "Brain cancer in the world: An epidemiological review," *World Cancer Res. J.*, vol. 6, p. 5, Jan. 2019.
[3] N. J. Goel, C. E. Bird, W. H. Hicks, and K. G. Abdullah, "Economic implications of the modern treatment paradigm of glioblastoma: An analysis of global cost estimates and their utility for cost assessment," *J. Med. Econ.*, vol. 24, no. 1, pp. 1018–1024, Jan. 2021.
[4] C. Rouse, H. Gittleman, Q. T. Ostrom, C. Kruchko, and J. S. Barnholtz-Sloan, "Years of potential life lost for brain and CNS tumors relative to other cancers in adults in the United States," *Neuro-Oncol.*, vol. 18, no. 1, pp. 70–77, Jan. 2016.
[5] B. H. Menze, "The multimodal brain tumor image segmentation benchmark (BRATS)," *IEEE Trans. Med. Imag.*, vol. 34, no. 10, pp. 1993–2024, Oct. 2015.
[6] U. Baid, S. Talbar, S. Rane, S. Gupta, M. H. Thakur, A. Moiyadi, N. Sable, M. Akolkar, and A. Mahajan, "A novel approach for fully automatic intra-tumor segmentation with 3D U-Net architecture for gliomas," *Frontiers Comput. Neurosci.*, vol. 14, p. 10, Feb. 2020.
[7] E. G. Van Meir, C. G. Hadjipanayis, A. D. Norden, H. K. Shu, P. Y. Wen, and J. J. Olson, "Exciting new advances in neuro-oncology: The avenue to a cure for malignant glioma," *CA, A Cancer J. Clinicians*, vol. 60, no. 3, pp. 166–193, May 2010.
[8] S. Bakas, H. Akbari, A. Sotiras, M. Bilello, M. Rozycki, J. S. Kirby, J. B. Freymann, K. Farahani, and C. Davatzikos, "Advancing the cancer genome atlas glioma MRI collections with expert segmentation labels and radiomic features," *Sci. Data*, vol. 4, no. 1, pp. 1–13, Sep. 2017.

[9] A. Khosravanian, M. Rahmanimanesh, P. Keshavarzi, and S. Mozaffari, "Fast level set method for glioma brain tumor segmentation based on superpixel fuzzy clustering and lattice Boltzmann method," *Comput. Methods Programs Biomed.*, vol. 198, Jan. 2021, Art. no. 105809.
[10] Z. Tang, S. Ahmad, P. Yap, and D. Shen, "Multi-atlas segmentation of MR tumor brain images using low-rank based image recovery," *IEEE Trans. Med. Imag.*, vol. 37, no. 10, pp. 2224–2235, Oct. 2018.
[11] H.-H. Chang and D. J. Valentino, "An electrostatic deformable model for medical image segmentation," *Computerized Med. Imag. Graph.*, vol. 32, no. 1, pp. 22–35, Jan. 2008.
[12] F. Yang, J. S. Suri, and M. Sonka, "Volumetric segmentation using shape models in the level set framework," in *Deformable Models*. Cham, Switzerland: Springer, 2007, pp. 161–207.
[13] A. Wadhwa, A. Bhardwaj, and V. S. Verma, "A review on brain tumor segmentation of MRI images," *Magn. Reson. Imag.*, vol. 61, pp. 247–259, Sep. 2019.
[14] A. Aslam, E. Khan, and M. M. S. Beg, "Improved edge detection algorithm for brain tumor segmentation," *Proc. Comput. Sci.*, vol. 58, pp. 430–437, Jan. 2015.
[15] D. H. Wu, "Machine learning paradigm for dynamic contrast-enhanced MRI evaluation of expanding bladder," *Frontiers Biosci.*, vol. 25, no. 9, pp. 1746–1764, 2020.
[16] S. Damodharan and D. Raghavan, "Combining tissue segmentation and neural network for brain tumor detection," *Int. Arab J. Inf. Technol.*, vol. 12, pp. 1–11, Jan. 2015.
[17] J. Zhang, Z. Jiang, J. Dong, Y. Hou, and B. Liu, "Attention gate ResU-Net for automatic MRI brain tumor segmentation," *IEEE Access*, vol. 8, pp. 58533–58545, 2020.
[18] A. Bhandari, J. Koppen, and M. Agzarian, "Convolutional neural networks for brain tumour segmentation," *Insights Into Imag.*, vol. 11, no. 1, pp. 1–9, Dec. 2020.
[19] L. Pei, L. Vidyaratne, M. M. Rahman, and K. M. Iftekharuddin, "Context aware deep learning for brain tumor segmentation, subtype classification, and survival prediction using radiology images," *Sci. Rep.*, vol. 10, no. 1, pp. 1–11, Nov. 2020.
[20] X. Xia and B. Kulis, "W-Net: A deep model for fully unsupervised image segmentation," 2017, *arXiv:1711.08506*.
[21] J. Amin, M. Sharif, M. Yasmin, and S. L. Fernandes, "Big data analysis for brain tumor detection: Deep convolutional neural networks," *Future Gener. Comput. Syst.*, vol. 87, pp. 290–297, Oct. 2018.
[22] S. Deepak and P. M. Ameer, "Brain tumor classification using deep CNN features via transfer learning," *Comput. Biol. Med.*, vol. 111, Aug. 2019, Art. no. 103345.
[23] M. B. Naceur, R. Saouli, M. Akil, and R. Kachouri, "Fully automatic brain tumor segmentation using end-to-end incremental deep neural networks in MRI images," *Comput. Methods Programs Biomed.*, vol. 166, pp. 39–49, Nov. 2018.
[24] F. J. Díaz-Pernas, M. Martínez-Zarzuela, M. Antón-Rodríguez, and D. González-Ortega, "A deep learning approach for brain tumor classification and segmentation using a multiscale convolutional neural network," *Healthcare*, vol. 9, no. 2, p. 153, Feb. 2021.
[25] T. Tamilvizhi, R. Surendran, K. Anbazhagan, and K. Rajkumar, "Quantum behaved particle swarm optimization-based deep transfer learning model for sugarcane leaf disease detection and classification," *Math. Problems Eng.*, vol. 2022, pp. 1–12, Jul. 2022.
[26] K. A. Ogudo, R. Surendran, and O. I. Khalaf, "Optimal artificial intelligence based automated skin lesion detection and classification model," *Comput. Syst. Sci. Eng.*, vol. 44, no. 1, pp. 693–707, 2023.
[27] S. Rajagopal, T. Thanarajan, Y. Alotaibi, and S. Alghamdi, "Brain tumor: Hybrid feature extraction based on UNet and 3DCNN," *Comput. Syst. Sci. Eng.*, vol. 45, no. 2, pp. 2093–2109, 2023.

SURENDRAN RAJENDRAN received the Ph.D. degree in computer science and engineering from Sathyabama University, in 2014. He is currently a Professor with the Department of Computer Science and Engineering, Saveetha School of Engineering, Saveetha Institute of Medical and Technical Sciences, India. His research interests include cloud computing, the Internet of Things, artificial intelligence, and big data.

SURESH KUMAR RAJAGOPAL is currently an Associate Professor with the Department of Center for System Design, Chennai Institute of Technology, Chennai, India. He has published several international journal and conference papers. His research interests include network security, data mining, machine learning, and web development.

TAMILVIZHI THANARAJAN received Ph.D. degree in computer science and engineering from the Sathyabama Institute of Science and Technology, in 2018. She is currently an Associate Professor with the Department of Computer Science and Engineering, Panimalar Engineering College, Chennai, India. Her research interests include cloud computing and big data.

K. SHANKAR (Senior Member, IEEE) received the Ph.D. degree in computer science from Alagappa University, Karaikudi, India. He is currently a Postdoctoral Fellow with the Big Data and Machine Learning Laboratory, South Ural State University, Russia, and an Adjunct Faculty of the Department of Computer Science and Engineering, Saveetha School of Engineering, Saveetha Institute of Medical and Technical Sciences, Chennai, India. He has authored/coauthored more than 150 ISI journal articles (with total Impact Factor more than 350) and more than 100 Scopus Indexed Articles. He has authored/edited six international books published by recognized publishers, such as Springer and CRC. His research interests include healthcare applications, secret image sharing scheme, digital image security, cryptography, the Internet of Things, and optimization algorithms.

SACHIN KUMAR (Senior Member, IEEE) received the Ph.D. degree in data mining/machine learning from the Indian Institute of Technology Roorkee, in 2017. He is currently associated with the Department of Computer Science, South Ural State University, Chelyabinsk, Russia. He is the Head of the Data Mining and Virtualization Laboratory and a Leading Researcher with the Big Data and Machine Learning Research Laboratory. He was a reviewer in various reputed international journals. His research interests include intelligent transportation systems, machine learning, data mining, the IoT, and health informatics.

NAJAH M. ALSUBAIE received the Ph.D. degree from the Department of Computer Science, University of Warwick, Coventry, U.K., in January 2019. During her Ph.D., she was a member of the Tissue Image Analytics (TIA) Laboratory. She collaborated with several parties, including Coventry hospitals, where she collected most of the data, and received her training on digital pathology. She is currently an Assistant Professor with Princess Nourah bint Abdulrahman University, Riyadh, Saudi Arabia. She has published several articles in histology image analysis. She was a reviewer for several articles.

MOHAMAD KHAIRI ISHAK (Member, IEEE) received the B.Eng. degree in electrical and electronics engineering from International Islamic University Malaysia (IIUM), Malaysia, the M.Sc. degree in embedded system from the University of Essex, U.K., and the Ph.D. degree from the University of Bristol, U.K. He is a Registered Graduate Engineer with the Board of Engineers Malaysia (BEM). He is currently a Senior Lecturer of mechatronics engineering with the School of Electrical and Electronic Engineering, Universiti Sains Malaysia (USM), where his background includes outstanding teaching experience, instructing students to stimulate engineering information interest and retention while invigorating classes through the use of new technologies and models. Emphasis is given towards the development of theoretical and practical methods which can be practically validated. Recently, significant research effort has been directed towards important industrial issues of embedded networked control systems and the IoT. His research interests include embedded systems, real-time control communications, and the Internet of Things (IoT).

SAMIH M. MOSTAFA received the bachelor's and M.Sc. degrees in computer science from the Computer Science-Mathematics Department, Faculty of Science, South Valley University, in 2004 and 2010, respectively, and the Ph.D. degree in computer science from the Advanced Information Technology Department, Graduate School of Information Technology, Kyushu University, Japan, in 2017. He is currently a fellow of the Academy of Scientific Research and Technology (ASRT), Egypt. His research interests include machine learning and CPU scheduling.